Contribution from the Department of Chemistry,
University of Delhi, Delhi-110007, India

Tetrahedrally Distorted Tetragonal Copper Complexes of a Tridentate Ligand

Gita Batra and Pavan Mathur*

Copper(II) complexes with a tridentate chelating ligand within the general 2 N, O donor class, containing a bis(benzimidazole) ether donor set, have been synthesized and characterized. Complexes of 1:1 stoichiometry form on mixing $Cu(ClO_4)_2 \cdot 6H_2O$ with the ligand in acetonitrile. X-band EPR spectra of the above complexes examined as a frozen acetonitrile solution indicate $g_{\parallel} > g_{\perp}$. The $g_{\parallel}$ and $A_{\parallel}$ values are consistent with the binding of less than three nitrogen atoms to the complex and border on Peisach and Blumberg plots of $A_{\parallel}$ vs $g_{\parallel}$ for two nitrogen and two oxygen atoms in the equatorial plane. Copper complexes of 1:2 stoichiometry form in the presesnce of an added exogenous ligand, viz. azide, acetate, and benzimidazole. X-Band EPR spectra of the above complexes indicate a severe distortion of the tetragonal symmetry. All of these show less than four $g_{\parallel}$ components and a broadening of the $g_{\perp}$ component. Superimposed on the broad $g_{\perp}$ component are eleven lines due to super hyperfine interaction (shf), with an average coupling constant of $B_N = 14 \pm 1$ G. Only in one case does the $m_I = -^3/_2$ component in the $g_{\parallel}$ region show well-resolved shf, with nine lines and $A_N = 11 \pm 1$ G, and the intensity pattern of the shf lines is in fair agreement with that observed for splitting due to four nitrogen atoms, i.e. 1:4:10:16:19:16:10:4:1. The intensity pattern of the shf lines on the $g_{\perp}$ component matches quite well with the ratios 1:4:11:20:29:32:29:20:11:4:1. Such a pattern is known to emerge if two sets of nine lines overlap to give an eleven-line pattern. In the present case the two sets of nine lines originate from overlapping of $g_{\parallel}$ and $g_{\perp}$ components. The fractions of s and p character (f_s and f_σ) have been evaluated for nitrogen bonding orbitals. We find that the ratio of f_s/f_σ is slightly lower than that expected for sp² hybridization, implying higher p character in the bonding orbitals of nitrogen atom. Molecular orbital coefficients β_1, β_2, and β'_1 have been evaluated after Maki and McGarvey. The trends of β_1 and β'_1 indicate increasing electron delocalization as we change the exogenous ligand from benzimidazole to acetate to azide, while the trend of $g_{\parallel}$ and $A_{\parallel}$ indicates marked tetrahedral distortion of the tetragonal site. The above complexes may have potential relevance to mononuclear copper sites in the turacin superoxide dismutase and to coordination geometries adopted by type 3 copper sites in rhus laccase and ascorbate oxidase.

Introduction

Chelating ligands incorporating benzimidazole groups have been extensively employed to synthesize and study copper complexes. One of the main reason for the use of such ligands has been prompted by studies which identify imidazole as one of the coordinating ligands in copper-containing proteins.[1-3] Moreover, benzimidazoles have nitrogen donor atoms which are sterically hindered, as they form part of the bulky benzimidazole groups; such a rigidity in the ligands enforces irregular geometric environments about the metals in their complexes, as can be imposed by the protein backbone structure. This is an added reason to synthesize and study copper complexes, as it has been suggested that most of the unusual redox properties of some copper enzymes are due to an unsymmetric metal environment.[4,5] Such an environment for the metal ion has been shown to be accessible through a variety of septadentate,[6] hexadentate,[7] tetradentate,[8] tripodal,[9] and tridentate[10] benzimidazole-based ligands. For the present study we have used a tridentate ligand[10] having two benzimidazole moieties and one ether oxygen as donor groups. We have further modified this ligand by attaching a *N*-butyl chain on N–H of the imidazole group. A preliminary communication about the synthesis of the ligand and its $Cu^{I}BF_4$ complex has been published[10a] earlier.

Experimental Section

Tetrahydrofuran was distilled from sodium. All other solvents were dried over molecular sieves. IR spectra were taken on a Shimadzu IR-435 spectrophotometer, X-band EPR spectra on a Jeol JES-FE 3XG ESR spectrometer with a variable-temperature liquid-nitrogen cryostat, and ¹H NMR spectra on a 90-MHz Perkin-Elmer R-32 instrument. Magnetic susceptibility was determined by the Evans[11] method at 300 K in acetonitrile-d_3 and DMSO-d_6. All other reagents and solvents were of commercially available reagent grade quality.

Preparation of $O(CH_2C_7H_5N_2)_2$ (DGB). A 12.1-g (90-mmol) amount of diglycollic acid was combined with 19.5 g (180 mmol) of *o*-phenylenediamine and powdered. The mixture was heated for about 3 h at a temperature of about 150 °C on a oil bath, till all effervescence ceases. The resulting red-blue glasslike solid after cooling was powdered and was added to 250 mL of 4 M HCl in small amounts. Upon scratching of the sides of the flask, a gray-white precipitate was obtained. This was filtered out and washed by slurrying in acetone several times. The above hydrochloride was dissolved in 200 mL of distilled water, and the resulting filtrate was then neutralized with 1:1 ammonia until a white precipitate was formed. This white precipitate was collected, washed with ether, and recrystallized from acetone: yield 14 g; mp 280–295 °C.

Preparation of N-Butylated DGB (BDGB). A 5-g sample of dried ligand (DGB) was suspended in dry tetrahydrofuran. This was stirred overnight with NaOH (1.4 g). Then butyl bromide (4 mL) was added, and the solution was left stirring for about 72 h. The solvents were stripped off, and the resulting residue was dissolved in chloroform and the solution filtered. To the filtrate was added *n*-hexane, and a yellow powder was deposited. This yellow powder was washed with hexane. The procedure adopted is similar to that of Reed et al.[6b]

DGB and BDGB were characterized by elemental analysis and ¹H NMR spectroscopy.

Anal. Calcd for $C_{16}H_{14}N_4O$ (DGB): C, 69.0; H, 5.0; N, 20.1. Found: C, 68.2; H, 4.7; N, 20.7. Calcd for $C_{24}H_{30}N_4O$ (BDGB): C, 73.8; H, 7.6; N, 14.3. Found: C, 72.9; H, 7.9; N, 13.6. ¹H NMR (DMSO-d_6) of $C_{16}H_{14}N_4O$: δ 7.7 (4 H, m), 7.3 (4 H, m), 4.95 (4 H, s). ¹H NMR (CCl₄) of $C_{24}H_{30}N_4O$: δ 7.5 (4 H, m), 7.05 (4 H, m), 4.6 (4 H, s), 3.95 (4 H, t), 1.55 (4 H, m), 1.65 (4 H, m), 0.7 (6 H, d).

(1) Tweedle, M. F.; Wilson, L. J.; Garcia-Iniquiz, L.; Babcock, G. T.; Palmer, G. *J. Biol. Chem.* **1978**, *253*, 8065.

(2) Brown, J. M.; Powers, L.; Kincaid, B.; Larrabee, J. A.; Spiro, T. G. *J. Am. Chem. Soc.* **1980**, *102*, 4210.

(3) (a) Eickman, N. C.; Solomon, E. J.; Larrabee, J. A.; Spiro, T. G.; Lerch, K. *J. Am. Chem. Soc.* **1978**, *100*, 6529. (b) Larrabee, J. A.; Spiro, T. G. *J. Am. Chem. Soc.* **1980**, *102*, 4217.

(4) (a) Solomon, E. I.; Hare, J. W.; Gray, H. B. *Proc. Natl. Acad. Sci. U.S.A.* **1976**, *73*, 1389 and references cited therein. (b) Vallee, B. L.; Williams, R. J. P. *Proc. Natl. Acad. Sci. U.S.A.* **1968**, *59*, 498.

(5) Holwerda, R. A.; Wherland, S.; Gray, H. B. *Annu. Rev. Biophys. Bioeng.* **1976**, *5*, 363.

(6) (a) Berends, H. P.; Stephan, D. W. *Inorg. Chem.* **1987**, *26*, 749–754. (b) Mckee, V.; Zvagulis, M.; Dagdigian, J. V.; Patch, M. G.; Reed, C. A. *J. Am. Chem. Soc.* **1984**, *106*, 4765–4772.

(7) (a) Birker, P. J. M. W. L.; Hendriks, H. M. J.; Reedijk, J.; Verschoor, G. C. *Inorg. Chem.* **1981**, *20*, 2408–2414. (b) Hendriks, H. M. J.; Birker, P. J. M. W. L.; Jacobus, V. R.; Verschoor, G. C.; Reedijk, J. *J. Am. Chem. Soc.* **1982**, *104*, 3607–3617.

(8) Birker, P. J. M. W. L.; Helder, J.; Krebs, B.; Henkel, G. *Inorg. Chem.* **1982**, *21*, 357–363.

(9) (a) Thompson, L. K.; Ramaswamy, B. S.; Dawe, R. D. *Can. J. Chem.* **1978**, *56*. (b) Hendriks, H. M. J.; Birker, P. J. M. W. L.; Verschoor, G. C.; Reedijk, J. *J. Chem. Soc., Dalton Trans.* **1982**, 623–631. (c) Addison, A. W.; Hendriks, H. M. J.; Reedijk, J.; Thompson, L. K. *Inorg. Chem.* **1981**, *20*, 103.

(10) (a) Berends, H. P.; Stephan, D. W. *Inorg. Chim. Acta* **1984**, *93*, 173–178. (b) Dagdigian, J. V.; Reed, C. A. *Inorg. Chem.* **1979**, *18*, 2623–2626.

(11) Evans, D. F. *J. Chem. Soc.* **1959**, 2003.
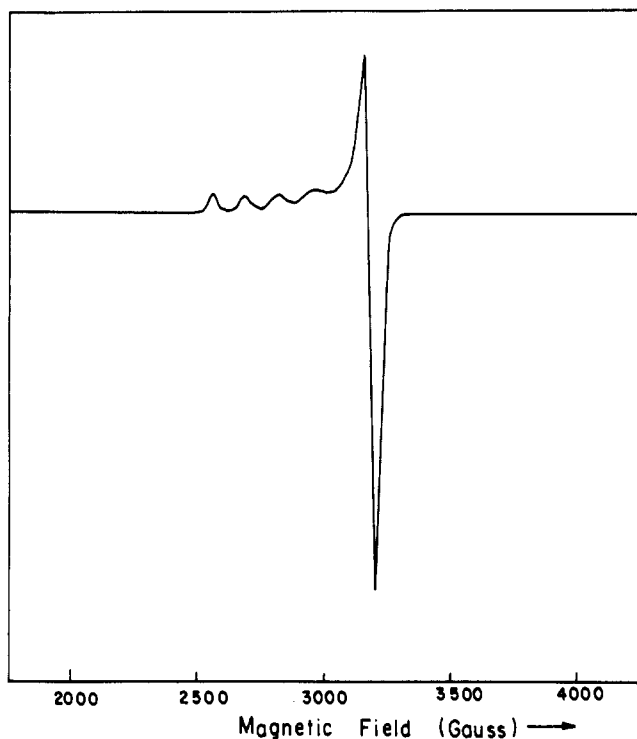
Figure 1. 5000-G scan of frozen acetonitrile solution of [Cu(BDGB)-(ClO$_4$)(H$_2$O)$_2$](ClO$_4$). Conditions: r. gain = 4 × 10^2; microwave power 10 mW; microwave frequency 9.2 GHz; 6.3-G modulation amplitude; T = 143 K at X-band and centered at 2500 G.
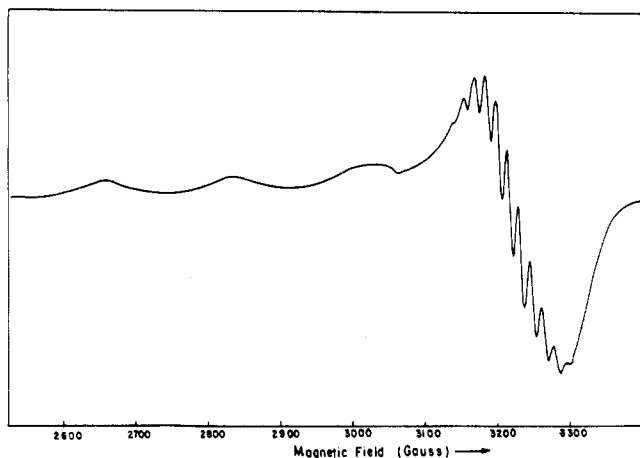
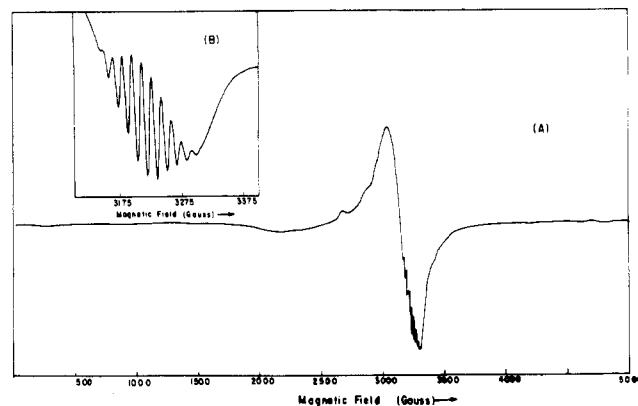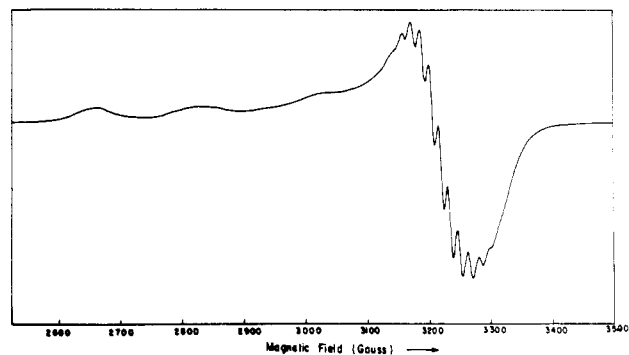**Figure 2.** 1000-G scan of the frozen DMF solution of [Cu(BDGB)$_2$-(ClO$_4$)(benz)(H$_2$O)](ClO$_4$)·2H$_2$O. Conditions: r. gain = 6.3 × 10; microwave power 10 mW; microwave frequency 9.2 GHz; 6.3-G modulation amplitude; T = 143 K at X-band.

Preparation of [Cu(BDGB)(ClO$_4$)(H$_2$O)$_2$](ClO$_4$). The ligand BDGB (0.33 mmol) was suspended in acetonitrile, and Cu(ClO$_4$)$_2$·6H$_2$O (0.33 mmol) solution (5 mL) in acetonitrile was added to the ligand mixture. Most of the ligand goes into solution, and the color changes from blue to green. This solution was stirred for about 1 h at room temperature. The solution was reduced to a small volume on a rotary evaporator, and a small amount of ether was added to precipitate the crude product. The product was washed and recrystallized with acetonitrile–ether mixture (1:5).

Anal. Calcd for C$_{24}$H$_{30}$N$_4$O(ClO$_4$)$_2$Cu·2H$_2$O: C, 41.8; H, 4.3; N, 8.1; Cu, 9.2. Found: C, 41.5; H, 4.9; N, 8.3; Cu, 9.9.

Preparation of Copper(II) Complexes Containing the Ligands DGB and BDGB and the Exogenous Ligands Azide, Acetate, and Benzimidazole. The ligand (0.66 mmol) was suspended in acetonitrile, and copper perchlorate (0.33 mmol) solution (5 mL) was added to the ligand suspension. Most of the ligand goes into solution. A 0.33-mmol portion of sodium azide, sodium acetate, and benzimidazole was added to each of the respective solutions. The blue color of the solution changes to green in azide and pinkish violet in the case of benzimidazole and acetate. After 20 min of stirring, a precipitate is formed. The resulting crude product

Figure 3. (A) 5000-G scan of [Cu(BDGB)$_2$(ClO$_4$)(OAc)]·2H$_2$O. Conditions: r. gain = 3.2 × 10^2; microwave power 10 mW; microwave frequency 9.2 GHz; 6.3-G modulation amplitude; T = 143 K at X-band. (B) 1000-G scan centered at 3125 G. Conditions: T = 143 K; r. gain = 3.2 × 10.

Figure 4. 1000-G scan of frozen DMF Solution of [Cu(BDGB)$_2$-(ClO$_4$)(N$_3$)]·H$_2$O. Conditions: r. gain = 6.3 × 10; microwave power 10 mW; microwave frequency 9.19 GHz; 6.3-G modulation amplitude; T = 143 K at X-band.
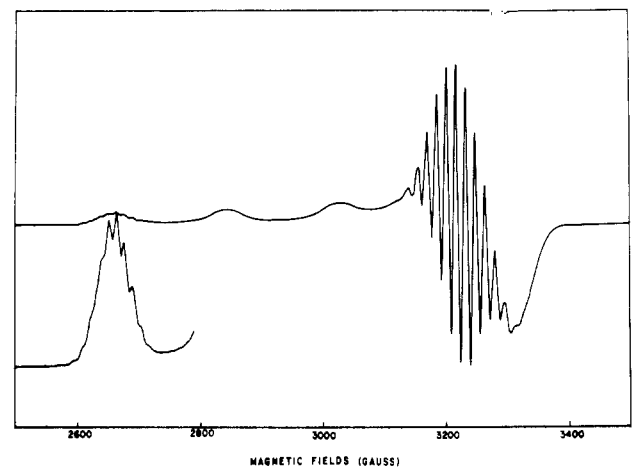
Figure 5. 1000-G scan of frozen DMF solution of [Cu(DGB)$_2$(ClO$_4$)-(benz)(H$_2$O)](ClO$_4$). Conditions: r. gain = 2.5 × 10 and resolved g at r. gain = 10 × 10; microwave power 10 mW; microwave frequency 9.2 GHz; 6.3-G modulation amplitude; T = 143 K at X-band.

was then washed with acetonitrile and recrystallized from a CH$_3$CN–DMF mixture.

Anal. Calcd for (C$_{24}$H$_{30}$N$_4$O)$_2$(ClO$_4$)$_2$(benzimidazole)Cu·3H$_2$O: C, 54.3; H, 5.3; N, 11.5; Cu, 5.2. Found: C, 53.9; H, 5.6; N, 10.6; Cu, 5.6. Calcd for (C$_{16}$H$_{14}$N$_4$O)$_2$(ClO$_4$)$_2$(benzimidazole)Cu·2H$_2$O: C, 48.1; H, 3.4; N, 14.3; Cu, 6.5. Found: C, 47.5; H, 3.3; N, 13.9; Cu, 6.2. Calcd for (C$_{24}$H$_{30}$N$_4$O)$_2$(ClO$_4$)(CH$_3$COO)Cu·2H$_2$O: C, 57.8; H, 6.4; N, 10.7; Cu, 6.1. Found: C, 56.7; H, 5.7; N, 9.8; Cu, 5.4. Calcd for (C$_{24}$H$_{30}$N$_4$O)$_2$(ClO$_4$)(N$_3$)Cu·H$_2$O: C, 57.4; H, 6.1; N, 15.3; Cu, 6.3. Found: C, 57.3; H, 5.4; N, 14.7; Cu, 6.1. Calcd for (C$_{16}$H$_{14}$N$_4$O)$_2$-(ClO$_4$)(N$_3$)Cu·2H$_2$O: C, 48.2; H, 4.0; N, 19.3; Cu, 7.9. Found: C, 47.2; H, 3.8; N, 19.7; Cu, 8.3.

Table I. X-Band EPR Spectral Data for Copper(II) Complexes[a]

| no.	complex	$g_\parallel$	$g_\perp$	$A_\parallel$	A_N	B_N	F_s	F_σ	F_s/F_σ	β'_1	β_1	β_2	α^2
1	[Cu(BDGB)(ClO₄)(H₂O)₂](ClO₄)	2.3764	2.06	137.5									0.63
2	[Cu(BDGB)₂(ClO₄)(benz)(H₂O)](ClO₄)·2H₂O	2.2374	2.03	180.0		14.1				0.59	0.86	0.9	0.59
3	[Cu(BDGB)₂(ClO₄)(OAc)]·2H₂O	2.2156	2.07	187.5		15.0				0.61	0.85	1.0	0.54
4	[Cu(BDGB)₂(ClO₄)(N₃)]·H₂O	2.2432	2.03	175.0		15.5				0.62	0.80	1.0	0.50
5	[Cu(DGB)₂(ClO₄)(benz)(H₂O)](ClO₄)·H₂O	2.2384	2.03	177.5	11.0	14.0	0.027	0.09	0.3	0.57	0.87	0.9	0.59
6	[Cu(DGB)₂(ClO₄)(N₃)]·2H₂O	2.2393	2.03	175.0		15.4				0.62	0.80	1.0	0.50
7	[Cu(DGB)₂(ClO₄)(N₃)]·2H₂O	2.27	2.02	187.5									

[a] Benz = benzimidazole.
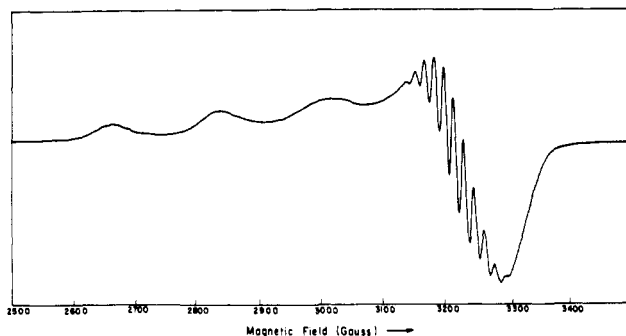
Figure 6. 1000-G scan of frozen DMF solution of [Cu(DGB)₂-(ClO₄)(N₃)]·2H₂O. Conditions: r. gain = 10 × 10; microwave power 10 mW; microwave frequency 9.2 GHz; 6.3-G modulation amplitude; T = 143 K at X-band.

Discussion

EPR Spectroscopy. Figures 1–6 illustrate the 9.50-GHz EPR spectra of copper(II) complexes, at 143 K, examined as a frozen acetonitrile or dimethylformamide solutions. In general, the EPR spectra reveal the presence of a distorted tetragonal copper site in the complexes. This is evident from the trend of their respective $g_\parallel$ and $g_\perp$ values, which in all cases shows $g_\parallel > g_\perp$ (data in Table I).

An examination of the $g_\parallel$ and $A_\parallel$ values for the complex [Cu(BDGB)(ClO₄)](H₂O)(ClO₄) indicates the highest value of $g_\parallel$ and the lowest $A_\parallel$ value in the series. This is consistent with binding of less than three nitrogen atoms to the complex and borders on Peisach and Blumberg plots of $A_\parallel$ versus $g_\parallel$ for two nitrogens and two oxygens in the equatorial plane.[12] Thus, EPR data support the presence of one tridentate ligand in the metal complex with other sites being occupied by coordinated ClO₄ and H₂O solvent molecules. No superhyperfine splittings from the ligand are observed (Figure 1).

An examination of EPR spectra of the remaining copper(II) complexes that have been prepared in the presence of added exogenous ligand reveals several features that are in sharp contrast to the above 1:1 complex of [Cu(BDGB)(ClO₄)(H₂O)₂](ClO₄). As per their stoichiometry, the remaining complexes are of 1:2 type. The EPR spectra of all these complexes clearly demonstrate a severe distortion of the tetragonal symmetry. All of them show less than four $g_\parallel$ lines and a broadening of the $g_\perp$ line (the $g_\perp$ line width at half-amplitude is twice that observed in the [Cu(BDGB)(ClO₄)(H₂O)₂](ClO₄) complex except for the acetato complex where only two $g_\parallel$ lines are observed and the $g_\perp$ line width is 4–5 times that of the 1:1 complex (Figure 3). Such a broadening of the $g_\perp$ component is indicative of lowered symmetry manifesting itself through a rhombic splitting.[13] Some of the EPR spectra of the 1:2 complexes are very similar to EPR X-band spectra observed for Cu–Zn superoxide dismutase[13a] while the EPR spectrum of the acetato complex has a striking similarity to that of the copper site in turacin.[13b]

An additional feature of the EPR spectra of 1:2 complexes is the observation of superhyperfine (SHF) splitting of the $g_\perp$
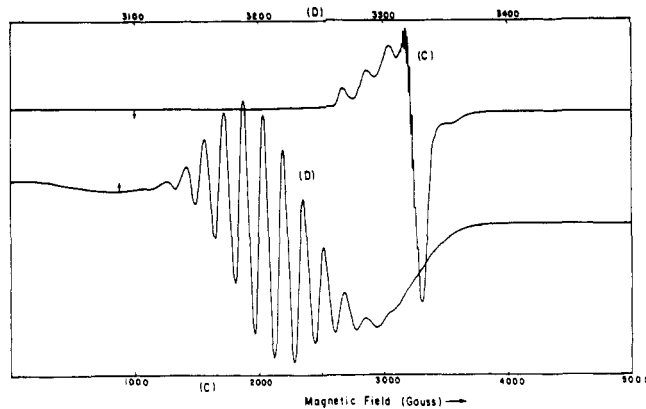

Figure 7. (C) 5000-G scan of frozen DMSO solution of [Cu(DGB)₂-(ClO₄)(N₃)]·2H₂O. Conditions: r. gain = 10 × 10²; microwave power 10 mW; microwave frequency 9.19 GHz; 6.3-G modulation amplitude; T = 143 K at X-band and centered at 2500 G. (D) 500-G scan centered at 3250 G. Conditions: T = 143 K; r. gain = 1.6 × 10².

component in all the cases (Figures 2–6). A clear 11-line pattern emerges in the $g_\perp$ component with $B_N \simeq$ 14–15 G (data in Table I).

The superhyperfine lines are not resolved on the $g_\parallel$ component except in the case of the [Cu(DGB)₂(ClO₄)₂(benz)] complex (benz = benzimidazole). Nine lines could be counted from the high-field side on the $m_I = -^3/_2$ component (Figure 5). These show inflections at the correct positions of progression (with A_N of 11 G), and the intensity pattern is in fair agreement with that observed for splitting due to four N atoms, which is 1:4:10:16:19:16:10:4:1.[15] The above predominantly isotropic SHF interaction is in accord with results obtained in other complexes containing the CuN₄ group in an approximately tetragonal crystal field.[14]

Two more inflections could be counted (beyond the nine lines) on the low-field side of the $m_I = -^3/_2$ component. More than nine lines have been observed even when only four N ligands are ligated to copper.[15a] However, an explanation is needed for the 11 SHF lines observed in the $g_\perp$ region where the intensity pattern does not match with that observed for the $g_\parallel$ part. We propose that this eleven-line pattern originates from the overlapping of two sets of nine lines each. One set of nine lines originates from the $g_\parallel$ component that overlaps with a second set of nine lines originating from the $g_\perp$ component. The intensities of 11 lines in all the cases matches quite well with the ratios 1:4:11:20:29:32:29:20:11:4:1. Such a intensity pattern for two sets of nine lines, merging into an eleven-line pattern has been observed for AgTPP in benzene.[16]

The above data clearly support the presence of two ligands per copper(II) in the above complexes with the four donor nitrogen atoms from benzimidazoles lying approximately in an equatorial plane. This is also supported by the crystal structure of a copper(II) complex with a similar tridentate benzimidazole ligand derived from iminodiacetic acid.[11a] In the 1:2 complexes one of

(12) Peisach, J.; Blumberg, W. E. *Arch. Biochem. Biophys.* **1974,** *165,* 69–708.

(13) (a) Weser, U.; et al. *Biochem. Biophys. Acta* **1971,** *243,* 203. (b) Blumberg, W. E.; Peisach, J. *J. Biol. Chem.* **1965,** *240,* 870.

(14) Bednarek, J.; Schlick, S. *J. Am. Chem. Soc.* **1990,** *112,* 5019–5024.

(15) (a) Assour, J. M. *J. Chem. Phys.* **1965,** *43,* 2477–2489. (b) Allen, H. C., Jr.; Kokoszka, G. F.; Inskeep, R. G. *J. Am. Chem. Soc.* **1964,** *86,* 1023.

(16) Manoharan, P. T.; Rogers, M. T. *Electron Spin Resonance of Metal Complexes*; Teh Fu Yen, Ed.; Plenum Press: New York, 1969.

the axial sites is occupied by one exogenous ligand, i.e. benzimidazole, azide, or acetate, and the other by ClO_4^- in the solid state. In solution, the coordinated perchlorate comes off as is indicated by conductance measurements and the sixth site in all probabilitiy is occupied by a weakly bound solvent molecule. The fact that the acetato complex also shows the same eleven-line SHF structure on the $g_\perp$ component as shown by corresponding benzimidazole and azide derivatives indicates that the nitrogen atom of the exogenous ligand in the latter two complexes does not interact strongly with the unpaired electron of copper(II). Since the solution EPR spectra are taken in DMF, to establish that the nitrogen atom of DMF does not contribute to the SHF interaction, we have taken X-band EPR spectra of one of the 1:2 complexes, $[Cu(DGB)_2(N_3)ClO_4)]$, in frozen DMSO-d_6 at 143 K (Figure 7). The EPR spectrum does not show any change in the number of SHF lines in the $g_\perp$ component, thus clearly suggesting no solvent effect. Thus, the origin of the SHF interaction is only from four nitrogen atoms from our two tridentate ligands.

However, there does occur a change in geometric configuration in the above complexes, as we change solvent from DMF to DMSO-d_6. This is apparent from an examination of the $g_\parallel$, $A_\parallel$ data (Table I) in both the solvents. A similar increase in $g_\parallel$, $A_\parallel$ values occurs for the analogous $[Cu(BDGB)_2(N_3)(ClO_4)]$ complex. This is indicative of the complex becoming increasingly ionic and planar in DMSO-d_6.

We have made an attempt to obtain MO coefficients for the b_{1g} and b_{2g} orbitals, i.e. β_1 and β_2, and also the ligand coefficient β'_1 in the b_{1g} MO. These have been evaluated from the expressions used by Manoharan and Rogers,[16] with $\phi^2(2s) = 33.4 \times 10^{24}$ cm^{-3} for the 2s function, and $\langle r^{-3} \rangle_p = 21.1 \times 10^{24}$ cm^{-1} for the 2p function following Maki and McGarvey[17] (Table 1). sp^2 hybridization in the bonding nitrogen orbitals has been assumed, although in one case, $[Cu(DGB)_2(benz)(ClO_4)_2]$, where it has been possible to obtain the fractions of s and p character (f_s and f_σ), we find that the ratio of f_s/f_σ is slightly lower than that expected for sp^2 hybridization (Table I). This could be interpreted in terms of higher p-character in the bonding orbitals presented by nitrogen toward copper atom and a tilt toward sp^3 hybridization. For calculation of the dipolar correction, a bond distance of 2.0 Å has been assumed. This Cu–N distance is in keeping with that found for other copper(II) benzimidazole[7a,8] complexes.

The data for β_1 and β'_1 are given in Table I. The values of β_1 and β'_1 are in keeping with those calculated for the Cu^{II}TPP complex and provide proof that there is considerable covalent bonding particularly in-plane σ bonding. The relative trend of β_1 and β'_1 with respect to the exogenous ligand shows that there is greater unpaired electron delocalization on the nitrogen atom as we move from benzimidazole–acetate to azide complexes.

The values for the in-plane π-bonding coefficient β_2 are given in Table I. The data suggest almost no in-plane π-bonding. Following Blumberg and Peisach, changing the axial ligand from the neutral benzimidazole to anionic acetate and azide in our 1:2 complexes leads to (i) overall decreased positive charge, while changing acetate ion to azide results in (ii) exchanging a less electron-rich O-atom to a more electron-rich nitrogen atom. Both these effects would tend to lower $g_\parallel$ and increase $A_\parallel$ as we move in the series benzimidazole, acetate, and azide. The effect of increasing covalency and distortion toward the tetrahedral arrangement of the equatorial ligands would oppose the above increase in $A_\parallel$ values along the series.

The present 1:2 complexes reflect a unique compensation of the above subtle electronic/structural effects. From benzimidazole to acetate, despite increased covalency (MO coefficients, α^2 data, Table I) and tetrahedral distortion (optical data), the lowered charge on the complex is the controlling effect leading to a relatively increased $A_\parallel$ lowered $g_\parallel$. However, as we move to the azide complex, increased tetrahedral distortion of the CuN$_4$ chromophore tends to be the dominant effect resulting in relatively increased $g_\parallel$ and lowered $A_\parallel$[18,19] (Table I).

Table II. Solution Magnetic Moment Data at 300 K

no.	compd	μ_{eff}/metal atom, ± 0.1 μ_B
1	$[Cu(BDGB)(ClO_4)(H_2O)_2](ClO_4)$	1.74
2	$[Cu(BDGB)_2(ClO_4)(benz)(H_2O)](ClO_4)\cdot 2H_2O$	1.79
3	$[Cu(BDGB)_2(ClO_4)(OAc)]\cdot 2H_2O$	1.83
4	$[Cu(BDGB)_2(ClO_4)(N_3)]\cdot H_2O$	2.09
5	$[Cu(DGB)_2(ClO_4)(benz)(H_2O)](ClO_4)\cdot H_2O$	1.75
6	$[Cu(DGB)_2(ClO_4)(N_3)]\cdot 2H_2O$	2.07

Table III. Optical Bands and Their Extinction Coefficients

compd	solvent	λ_{max}, nm	log ϵ
DGB	ethanol	252	4.14
		272	4.23
		282	4.18
$[Cu(DGB)_2(ClO_4)(benz)(H_2O)](ClO_4)\cdot H_2O$	DMF	272	5.93
		284	5.87
		600	2.03
$[Cu(DGB)_2(ClO_4)(N_3)]\cdot 2H_2O$	DMF	276	4.23
		284	4.20
		404	2.93
		700	1.88
BDGB	methanol	258	4.19
		277	4.18
		286	4.13
$[Cu(BDGB)(ClO_4)(H_2O)_2](ClO_4)$	acetonitrile	240	4.18
		264	4.28
		272	4.27
		756	1.29
$[Cu(BDGB)_2(ClO_4)(benz)(H_2O)](ClO_4)\cdot 2H_2O$	DMF	274	5.85
		283	5.62
		574	1.98
$[Cu(BDGB)_2(ClO_4)(OAc)]\cdot 2H_2O$	DMF	273	4.17
		281	4.18
		634	1.99
$[Cu(BDGB)_2(ClO_4)(N_3)]\cdot H_2O$	DMF	275	4.44
		284	4.49
		400	3.09
		712	2.08

Magnetic Susceptibility. The magnetic susceptibilities of copper(II) complexes in solution were determined by the Evans method[11] at 300 K in acetonitrile-d_3 for $[Cu(BDGB)-(ClO_4)(H_2O)_2](ClO_4)$ and in DMSO-d_6 for other copper(II) complexes having an exogeneous ligand. The diamagnetic corrections for each complex were estimated using Pascal's constants and were incorporated in the experimental solution susceptibility.

The experimental magnetic moments of all the copper(II) complexes are given in the Table II and lie within the range as normally found for other copper(II) complexes.

The relatively higher magnetic moments of the azido complexes in the above series could be rationalized in terms of a decreased 3d–4p orbital mixing. This happens as the tetrahedrally distorted azido complexes become more planar (centrosymmetric) in DMSO-d_6. This is supported by comparing their $g_\parallel$ and $A_\parallel$ values in DMF and DMSO-d_6, respectively.

Electronic and IR Spectroscopy. The ligands and their copper(II) complexes show characteristic UV spectra of a benzimidazolyl group. The absorption bands and their respective extinction coefficients are reported in Table III.

The UV bands are in general blue shifted upon coordination and in some cases enhanced in intensity as evidenced by extinction coefficients. This includes the band at 258 nm in BDGB, which is associated with the imidazole ring showing clear evidence of C=N coordination to the copper site in the $[Cu(BDGB)-(ClO_4)(H_2O)_2](ClO_4)$ complex. Similar binding is expected in other complexes.

All the copper complexes exhibit one major absorption in the range 550–850 nm (i.e. 18 000–11 750 cm^{-1}). Band maxima (λ_{max}) values are tabulated in Table III and shown in Figure 8. The large molar extinction coefficients of these complexes ranging from 120 to 75 M^{-1} cm^{-1} indicate that the copper site in the complexes

(17) Maki, A. H.; McGarvey, B. R. *J. Chem. Phys.* **1958**, *29*, 1.
(18) Sakaguchi, U.; Addison, A. W. *J. Chem. Soc., Dalton Trans.* **1979**, 600.

(19) Seebauer, E. G.; Duliba, E. P.; Scogin, D. A.; Gennis, R. B.; Belford, R. L. *J. Am. Chem. Soc.* **1983**, *105*, 4926.
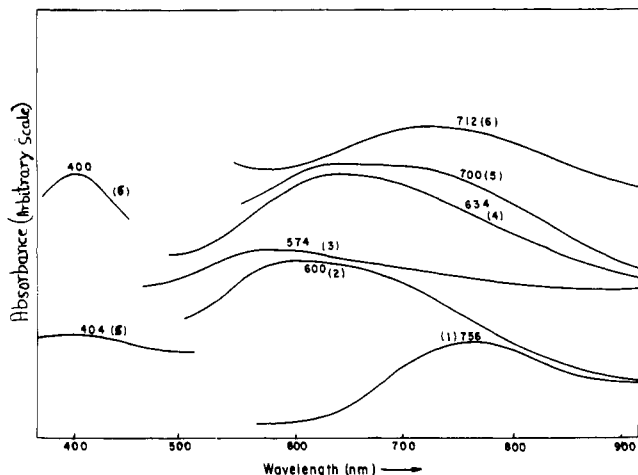
Figure 8. Optical spectra in the range 350–900 nm of the following complexes: (1) [Cu(BDGB)(ClO₄)(H₂O)₂](ClO₄); (2) [Cu(DGB)₂-(ClO₄)(benz)(H₂O)](ClO₄)·H₂O; (3) [Cu(BDGB)₂(ClO₄)-(benz)(H₂O)](ClO₄)·2H₂O; (4) [Cu(BDGB)₂(ClO₄)(OAc)]·2H₂O; (5) [Cu(DGB)₂(ClO₄)(N₃)]·2H₂O; (6) [Cu(BDGB)₂(ClO₄)(N₃)]·H₂O.

is of lower symmetry. Utilizing the energy ranges covered by the d–d transitions (λ_{max}) of CuN_{4-6} chromophores of different stereochemistry,[20] one concludes that in the present case the CuN_5 chromophore containing complexes (with benzimidazole and an azide group) fall in the class of distorted square-based pyramidal, the distortion being toward a tetrahedral arrangement of the equatorial ligands, while the CuN_4 chromophore containing acetato complex falls in the general category of a compressed tetrahedron.

The azide complexes, i.e. [Cu(DGB)₂(ClO₄)(N₃)]·2H₂O and [Cu(BDGB)₂(ClO₄)N₃)]·H₂O, show a charge-transfer band at 404 (ϵ = 867 M⁻¹ cm⁻¹) and at 400 nm (ϵ = 1250 M⁻¹ cm⁻¹) along with the d–d bands at 700 (ϵ = 76.25 M⁻¹ cm⁻¹) and 712 nm (ϵ = 120.55), respectively. The charge-transfer bands are absent in the corresponding acetato and benzimidazole. Our results indicate that axial-bound azide would also show a charge-transfer transition; this is at variance with results reported earlier.[21] The bands in the azide complexes compare well with the bands of similar energy in methemocyanin (N₃) (*Basycon canaliculatum*) at 360 (ϵ = 1580) and 710 nm (ϵ = 200).[21]

We have calculated α^2 by using a simple relationship:[22]
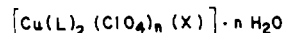
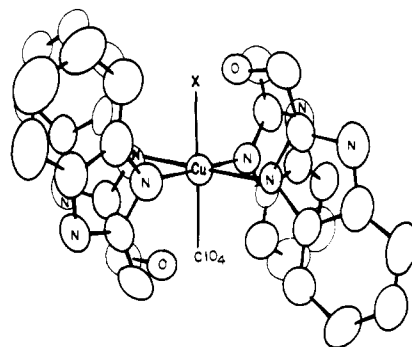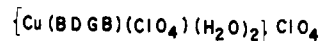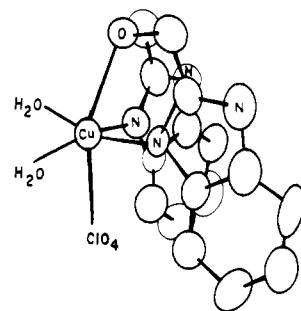$$g_{\parallel} = 2.0023 - 8\lambda\alpha^2/xy$$

The value of α^2 is given in Table I. The quantity α^2 is a function which depends on the nature of the copper–ligand bond, decreasing with increasing covalency to a minimum theoretical value of 0.50. It is found that the order of decreasing covalency is azide > acetate > benzimidazole for the copper(II) complexes containing these ligands and is in conformity with the order obtained from MO coefficients.

IR spectra were taken in Nujol mulls. In the free ligand a strong band appears at 1450–1460 cm⁻¹. On the basis of the analogy with the assigned bands for imidazole, the 1460-cm⁻¹ band is attributable to (C=N–C=C–). In our case, we find that the shift is of the order of 10–35 cm⁻¹ in the complexes (Table IV). This implies direct coordination of all the imine nitrogen atoms to copper(II).[23]

The copper complexes containing azide and acetato groups show a doublet in the region 1040–1120 cm⁻¹. This is assigned to the splitting of the ν_3(ClO₄⁻) band, into two components, indicating a coordinated ClO₄⁻ anion in the above cases. In the rest of the complexes, besides a splitting of the ν_3(ClO₄⁻) band, a strong

Table IV. Observed IR Frequencies (cm⁻¹) and Proposed Modes of Assignments for the Ligand and Complexes

DGB	[Cu(DGB)₂(ClO₄)(benz)(H₂O)](ClO₄)·H₂O	[Cu(DGB)₂-(ClO₄)(N₃)]·2H₂O	assgnt
	3300	3300	$\nu_{(N-H)}$, $\nu_{(O-H)}$
		2000	ν_{asym}(N=N=N)
		2050	
1620	1620	1620	(C=N)
	1485	1500	
1460	1450	1440	(C=N–C=C–)
	1120	1120	E \} ν_3(ClO₄⁻)
	1040	1040	A₁ \} unidentate
	1100		$\nu_{3(ClO4^-)}$ ionic

BDGB	[Cu(BDGB)-(ClO₄)(H₂O)₂-(ClO₄)]	[Cu(BDGB)₂-(ClO₄)(benz)]-(ClO₄)·2H₂O	assgnt
	3500	3200	$\nu_{(N-H)}$, $\nu_{(O-H)}$
1610	1610	1605	(C=N)
1455	1485	1485	(C=N–C=C–)
	1460	1450	
	1120	1110	E \} ν_3(ClO₄⁻) unidentate
	1020	1030	A₁ \}
	1080	1080	$\nu_{3(ClO4^-)}$ ionic

	[Cu(BDGB)₂-(ClO₄)(OAc)]·2H₂O	[Cu(BDGB)₂-(ClO₄)(N₃)]·H₂O	assgnt
	3400	3400	$\nu_{(N-H)}$, $\nu_{(O-H)}$
		2010	
		2090	ν_{asym} (N=N=N)
	1580	1610	(C=N)
	1480	1485	(C=N–C=C–)
	1450	1450	
	1140	1130	E \} ν_3(ClO₄⁻) unidentate
	1140	1020	A₁ \}

{Cu(BDGB)(ClO₄)(H₂O)₂} ClO₄

[Cu(L)₂ (ClO₄)ₙ (X)]·n H₂O

L = DGB & BDGB

X = N₃⁻, OAc⁻, Benz.

Figure 9. Proposed structures of the copper(II) complexes.

singlet is observed at around 1080 cm⁻¹. This indicates the presence of both coordinated and ionic perchlorate groups.[9a] The azide complexes additionally show bands in the region of 2000 cm⁻¹, and the antisymmetric stretch ν_3(N₃⁻) is split into a doublet

(20) Hathaway, B. J. *J. Chem. Soc., Dalton Trans.* **1972**, 1196.
(21) Himmelwright, R. S.; Eickman, N. C.; LuiBien, C. D.; Solomon, E. I. *J. Am. Chem. Soc.* **1980**, *102*, 5378–5388.
(22) Grawford, T. H.; Dalton, J. O. *Arch. Biochem. Biophys.* **1969**, *131*, 123–128.
(23) (a) Mathur, P.; Crowder, M.; Dismukes, G. C. *J. Am. Chem. Soc.* **1987**, *109*, 5227. (b) Tripathi, A. K.; Sharma, K. K.; Mathur, P. *Ind. J. Chem.* **1991**, *30A*, 400–405.

(Table IV) indicating that the azido group is nonlinearly coordinated to Cu(II).[24]

There is a broad absorption in the range 3200–3600 cm^{-1} associated with the N–H stretch and coordinated/lattice water.

IR data support the stoichiometry/structure proposed for the above complexes (Figure 9).

(24) Forster, D.; Horrocks, W. D. *Inorg. Chem.* **1966**, *5*, 1510–1514.

Contribution from the Department of Chemistry, School of Science and Engineering, Waseda University, Shinjuku-ku, Tokyo 169, Japan

Surface-Enhanced Resonance Raman Scattering Study on the Axial Ligation States of Manganese and Chromium Tetraphenylporphines Adsorbed on Silver Electrode Surfaces

Tatsushi Okumura, Shigeru Endo, Akio Ui, and Koichi Itoh*

Surface-enhanced resonance Raman scattering spectra (SERRS) in the region below 500 cm^{-1} were recorded for the manganese(III) and chromium(III) tetraphenylporphine complexes (TPP)Mn^{III}X (X = Cl$^-$, ClO$_4^-$) and (TPP)Cr^{III}X (X = Cl$^-$, ClO$_4^-$) adsorbed on a silver electrode surface in acetonitrile (ACN). The surface spectra in the low-frequency region clearly reflect changes in the axial ligation states of the metalloporphines associated with the adsorption process involving the silver electrode. On adsorption to the electrode at 0 V (vs Ag/AgCl), (TPP)Mn^{III}Cl dissociates the fifth axial ligand (a chloride ion), forming an adsorbed species, [(TPP)Mn^{III}]$^+$. On the other hand, (TPP)Cr^{III}Cl retains the chloride ion as a fifth axial ligand on the electrode surface at 0 V. Upon a negative sweep of the electrode potential, the chloride complex gradually disappears, forming [(TPP)Cr^{III}]$^+$; the disappearance is completed at –0.4 V. A SERRS spectrum obtained for a divalent manganese TPP complex adsorbed on a silver electrode proved that the adsorbate is a four-coordinated species; in contrast, the divalent manganese complex in ACN exists as a five-coordinated complex possessing an associated solvent molecule as a fifth ligand (i.e., (TPP)Mn^{II}(ACN)).

Introduction

Surface-enhanced resonance Raman scattering (SERRS) spectroscopy has been recognized as one of the most sensitive techniques to observe the vibrational spectra of various chromophores,[1–3] including heme proteins[4–8] and chlorophylls[9,10] adsorbed on coinage metals such as silver and gold. Its high sensitivity permits acquisition of the vibrational spectra of adsorbates even at a surface coverage less than a monomolecular layer. Surface spectra have been measured also for synthetic metalloporphines adsorbed on silver electrodes,[11–14] silver colloids,[15] and roughened silver surfaces;[16] the results revealed characteristic features of their surface processes including redox reactions and metal-insertion and -exchange reactions.

In the present paper, we report the SERRS spectra of adsorbates on a silver electrode for manganese(III) and chromium(III) tetraphenylporphines having an axially coordinated monoanion, such as chloride and perchlorate, in acetonitrile (ACN); the

manganese and chromium complexes are abbreviated as (TPP)Mn^{III}X (X = Cl$^-$, ClO$_4^-$) and (TPP)Cr^{III}X (X = Cl$^-$, ClO$_4^-$), respectively. The SERRS spectra were also recorded for (TPP)Mn^{II} and (TPP)Cr^{II}, which were electrochemically generated on the surface from the corresponding trivalent complexes. During the analysis of the surface spectra, we confined our attention to the elucidation of changes in the ligation states of the metalloporphines caused by adsorption to the silver electrode surface. With regard to the ligation states in solutions, electrochemical, spectrophotometric, and conductometric studies have been performed on the manganese[17] and chromium[18–20] complexes, revealing the following points. (i) (TPP)Mn^{III}ClO$_4$ and (TPP)Cr^{III}ClO$_4$ dissociate the perchlorate ion in ACN, forming [(TPP)Mn^{III}]$^+$ and [(TPP)Cr^{III}]$^+$, respectively. (ACN may associate with the manganese and chromic complexes, forming [(TPP)Mn^{III}(ACN)$_2$]$^+$ and [(TPP)Cr^{III}(ACN)$_2$]$^+$, respectively. Actually, this type of six-coordination state has been postulated for the trivalent complexes in dimethylformamide and pyridine, which are more strongly coordinating solvents than ACN.[17,19] In this paper, however, the coordination of ACN to the trivalent complexes is neglected because we have not obtained direct evidence for the coordination.) (ii) (TPP)Mn^{III}Cl and (TPP)Cr^{III}Cl in ACN retain the chloride ion as a fifth axial ligand. On the other hand, no direct measurement has been performed to clarify the ligation states of the manganese and chromium complexes adsorbed on electrode surfaces. A clarification of the ligation states of the metalloporphines adsorbed on the electrode surfaces is of crucial importance to the analysis of their electrochemical properties, because an electron transfer should take place between the adsorbates and the electrode surfaces during the redox reactions of the complexes. From comparison of the SERRS and RRS spectra of the trivalent and divalent complexes, we found that the SERRS features in the low-frequency region (below 500 cm^{-1})

(1) Van Duyne, R. P. In *Chemical* and *Biological Application of Lasers*; Moore, C. B., Ed.; Academic Press: New York, 1979; Vol. 4, Chapter 5.
(2) Moskovits, M. *Rev. Mod. Phys.* **1985**, *57*, 783.
(3) Cotton, T. M. In *Spectroscopy of Surfaces*; Clark, R. J., Hester, R. E., Eds.; John Wiley & Sons: Chichester, U.K., 1988; Chapter 3.
(4) Cotton, T. M.; Schultz, S. G.; Van Duyne, R. P. *J. Am. Chem. Soc.* **1980**, *102*, 7960.
(5) Copeland, R. A.; Foder, S. P. A.; Spiro, T. G. *J. Am. Chem. Soc.* **1984**, *106*, 3872.
(6) Smulvevich, G.; Spiro, T. G. *J. Phys. Chem.* **1985**, *89*, 5168.
(7) Hildebrandt, P.; Stockburger, M. *J. Phys. Chem.* **1986**, *90*, 6017.
(8) de Groot, J.; Hester, R. E.; Kaminaka, S.; Kitagawa, T. *J. Phys. Chem.* **1988**, *92*, 2044.
(9) Cotton, T. M.; Van Duyne, R. P. *FEBS Lett.* **1982**, *147*, 81.
(10) Hildebrandt, P.; Spiro, T. G. *J. Phys. Chem.* **1988**, *92*, 3355.
(11) Cotton, T. M.; Schultz, S. G.; Van Duyne, R. P. *J. Am. Chem. Soc.* **1982**, *104*, 6528.
(12) Itabashi, N.; Kato, K.; Itoh, K. *Chem. Phys. Lett.* **1983**, *97*, 528.
(13) Koyama, T.; Yamaga, M.; Kim, M.; Itoh, K. *Inorg. Chem.* **1985**, *24*, 4258.
(14) Sanchez, L. A.; Spiro, T. G. *J. Phys. Chem.* **1985**, *89*, 753.
(15) Itoh, K.; Sugii, T.; Kim, M. *J. Phys. Chem.* **1988**, *92*, 1568.
(16) Kobayashi, Y.; Itoh, K. *J. Phys. Chem.* **1985**, *89*, 5174.

(17) Kelly, S. L.; Kadish, K. M. *Inorg. Chem.* **1982**, *21*, 3631.
(18) Summerville, D. A.; Jones, R. D.; Hoffman, B. M.; Basolo, F. *J. Am. Chem. Soc.* **1977**, *99*, 8195.
(19) Bottomley, L. A.; Kadish, K. M. *Inorg. Chem.* **1983**, *22*, 342.
(20) Kelley, S. L.; Kadish, K. M. *Inorg. Chem.* **1984**, *23*, 679.